



Torres, R. B., dos Santos, J. C., Panzera, T. H., Christoforo, A. L., Ribeiro Borges, P. H., & Scarpa, F. (2017). Hybrid glass fibre reinforced composites containing silica and cement microparticles based on a design of experiment. *Polymer Testing*, 57, 87-93.
<https://doi.org/10.1016/j.polymertesting.2016.11.012>

Peer reviewed version

License (if available):
Unspecified

Link to published version (if available):
[10.1016/j.polymertesting.2016.11.012](https://doi.org/10.1016/j.polymertesting.2016.11.012)

[Link to publication record in Explore Bristol Research](#)
PDF-document

This is the accepted author manuscript (AAM). The final published version (version of record) is available online via Elsevier at <http://dx.doi.org/10.1016/j.polymertesting.2016.11.012>. Please refer to any applicable terms of use of the publisher.

University of Bristol - Explore Bristol Research

General rights

This document is made available in accordance with publisher policies. Please cite only the published version using the reference above. Full terms of use are available:
<http://www.bristol.ac.uk/red/research-policy/pure/user-guides/ebr-terms/>

HYBRID GLASS FIBRE REINFORCED COMPOSITES CONTAINING SILICA AND CEMENT MICROPARTICLES BASED ON A DESIGN OF EXPERIMENT

Rubens Bagni Torres¹, Júlio Cesar dos Santos¹, Túlio Hallak Panzera^{1*}, André Luiz

Christoforo², Paulo H Ribeiro Borges³, Fabrizio Scarpa⁴

(*corresponding author)

^{1*}Centre for Innovation and Technology in Composite Materials - CIT^cC, Department of Mechanical Engineering/Department of Natural Sciences, Federal University of São João del-Rei, Brazil. Tel/Fax: +55(32)33792603, panzera@ufsj.edu.br.

²Department of Civil Engineering, Federal University of São Carlos, Brazil.

³Federal Centre for Technological Education of Minas Gerais, Department of Civil Engineering, Brazil.

⁴Advanced Composites Centre for Innovation and Science, University of Bristol, UK.

Abstract

Hybrid Glass Fibre Reinforced Composites (HGRFCs) made with unidirectional glass fibres and silica or cement microparticles inclusions were investigated in order to improve their performance under flexural and impact loadings. Two full factorial designs were conducted to evaluate (i) the effect of the particle weight fraction on the compressive modulus of epoxy polymer (2^{13^1}) and (ii) the effect of the number of layers and type of particle (3^2) on the apparent density, flexural modulus and strength of HGRFCs. Composites with higher flexural properties were evaluated under impact loading via one-way analysis. TGA and FTIR analyses were used to verify the effect of ceramic particles within the polymeric phase. A microstructural analysis (SEM) was performed to verify the fracture mode and better assess the mechanical performance of HGRFCs.

Key words: hybrid composite; silica particle; Portland cement; glass fibre; three-point bending test; impact resistance.

1 Introduction

Glass fibre reinforced composites (GFRCs) have been widely used in many engineering applications such as automotive, aeronautics and civil construction, combining high specific strength/stiffness, thermal stability and lower cost material compared to carbon and aramid fibres [1]. The brittle nature of most fibre reinforced composites (FRCs) plays an important role in progressive failure mode and energy absorption capability of composite structures [2].

One way to enhance the mechanical properties of fibre reinforced composites (FRCs) is to improve the properties of the epoxy matrix phase by adding micro or nano-particle inclusions [3], being referred to as hybrid fibre reinforced composites (HFRCs) [4]. Particular types of particle-reinforcement have been proposed in open literature, including hybridization through micro-scaled [5] and nano-scaled inclusions (i.e. carbon nanotubes, graphene sheets, alumina, titanium oxide and silica particles [6-9]). The mechanical enhancement of HFRCs has been attributed to the interaction between fibres and particle-reinforced polymer [10]. In the case of silica particle inclusions, unsaturated bonds and various hydroxide groups can contribute to enhance the adhesion between the fibre and the matrix phase [11].

Impact damage is considered to be a primary cause of in-service delamination in composites, which can reduce the residual strength by as much as 60%. In fact, the poor tolerance to accidental low velocity impact of composite laminates is still a limitation to their use in many applications. An improvement of impact resistance by adding particle inclusions along with no degrading of flexural properties has been reported in the literature [12-14].

Detomi *et al.* [15] have reported the flexural behaviour of hybrid glass fibre reinforced composites with silicon carbide and silica particles incorporated at the upper beam side of the laminate. An increase in flexural strength and specific strength up to 110% and 112%, respectively, were achieved compared to the glass fibre reinforced composite. The use of ceramic particles at the compressive beam side under bending loadings contributes to enhancing the stiffness of the matrix phase, consequently compensating for the low compressive strength of the fibres.

The incorporation of Portland cement particles into epoxy polymer led to an increase of stiffness and toughness under compressive loading. Hydrated cement products have been found inside the epoxy polymer with no water addition. The

mechanical enhancement was attributed to the presence of stiff hydrated cement grains and secondary bonds (hydrogen bonds) [16].

Based on the achievements previous reported [15, 16], a hybrid glass fibre reinforced composite (HGFRC), containing cement or silica microparticles at the compressive beam side, was assessed by apparent density, impact resistance and three-point-bending test.

2 Materials and Methods

Unidirectional glass-fibre fabric (107 g/cm^2) was supplied by Owens Corning-Brazil, while the epoxy resin (RenLam M) and the hardener (HY 956) were provided by Huntsman-Brazil. The silica microparticles were sourced from Moinhos Gerais Company (Brazil), while the cement microparticles were supplied by Holcim Company (Brazil).

Experiment I consisted of a full factorial design ($2^1 3^1$) to investigate the effect of microparticle types (cement and silica) and their particle weight fractions (3, 5 and 10wt%) on the compressive modulus of particle-reinforced epoxy polymer (Table 1). The microparticles were classified in monomodal size at $37\mu\text{m}$ using a laboratory sieve. Subsequently, the particles were hand-mixed with the epoxy polymer for 5 minutes. Silicone cylindrical moulds were used to obtain the specimens for the compression testing based on the recommendations of ASTM 695 [17].

[Table 1]

Experiment II was conducted based on a full factorial design (3^2) to evaluate the effect of the factors, number of layers (7, 9 and 11) and particle inclusions (0wt% and 5wt% of cement and silica) on the apparent density, impact resistance, flexural modulus and strength of HGFRCs (Table 2). The volume fraction of fibres (30%) and the weight fraction of particles (5wt%) were considered constant in the experiment based on the results of preliminary tests. The laminates were fabricated using a hand lay-up method at room-temperature ($25\pm 1^\circ\text{C}$). The dispersive phases consisted of unidirectional glass fibres and silica or cement microparticles. The particles were hand-mixed with the epoxy resin for 5 minutes, and then used to laminate the layers placed above the neutral axis of the composite beam. A pristine epoxy polymer was used to laminate the layers placed under the neutral axis of the composites. It is well known the hydrated cement paste increases strength as a function of time up to nearly 28 days [18]. Therefore, in

order to avoid non-controlled factors in the experiment, the cure time of 28 days was used. A randomization procedure was adopted during the sample fabrication and the experimental tests. Five samples were produced for each experimental condition, and two replicates were carried out over a total of 90 specimens. The samples were placed into a plastic container to protect the specimens from humidity during the cure time. A replicate consists of repeating the experimental condition (E.C.), making possible, therefore, to estimate the experimental error related to the individual response [19].

Flexural and impact tests were carried out according to ASTM D790 [20] and ASTM 6110 [21] standards to determine the flexural strength and modulus and impact resistance of the composites. The apparent density was calculated based on the recommendations of ASTM D792 [22] using a precision balance (0.001 g) and distilled water at 25°C. A tensile machine Shimadzu AG-X Plus with a 100kN load cell and an impact test machine XJJ-50 Series were used to perform the three-point bending test and impact resistance, respectively. The impact tests were only conducted on 11 layer composites made of 5wt% of particles (silica or cement), that achieved higher flexural mechanical properties.

[Table 2]

[Table 3]

3. Results

3.1 Experiment I. Particle reinforced epoxy polymer

Table 1 shows the mean compressive modulus for replicate 1 and 2. The interaction of the factors significantly affected the response, showing a P-value lower than 0.05 (Table 3). Figure 1 shows the interaction effect plot of the factors Type of particle and Particle inclusion for the mean compressive modulus. Cement particles achieved higher modulus compared to silica inclusions for all particle weight fractions. Both microparticles provided superior stiffness when 5wt% of particle inclusions was considered. A percent increase of 67% was achieved compared to the baseline pristine condition (polymer without particle inclusions). Panzera *et al.* [16] have found a significant increase in mechanical properties of Portland cement-reinforced epoxy polymers. The mechanical enhancement was attributed to the presence of hydrated cement products (Figure 2) which stiffens the epoxy polymer.

[Figure 1]

MEV/EDS analyses were performed on an epoxy polymer with Portland cement inclusions. Figure 2(a) shows a backscattering electron image, which reveals the cement particles are well distributed in the polymer. A higher magnification image (1000×) is shown in Figure 2b, which was analysed via EDS technique. The cement particles consist of some clinker elements (non-hydrated products) such as, calcium, silica, oxygen, aluminium and magnesium (probably calcium silicates and aluminates). The presence of carbon reveals the epoxy polymer matrix phase (Figure 2c and 2d).

In polymers, a cross-link effect is considered a bond technique that links one polymer chain to another, being used to enhance the polymer stiffness. This effect can be achieved by chemical (covalent and ionic) or only physical bonds. A stiffness increase was achieved when the polymer was embedded with ceramic particles (Figure 1). In order to better assess the presence of cross-link bonds, TGA and FTIR analyses were conducted.

[Figure 2]

3.2 Thermogravimetric (TGA) and Infrared Spectroscopy (FTIR) analyses

The mechanical properties of epoxy polymer are often linked directly to its crosslink density. Some changes in crosslink density invariably lead to changes in mechanical properties [23].

The TGA curves of pristine epoxy, silica/epoxy, and cement/epoxy at a heating rate of 20 C/min indicate the epoxy and silica/epoxy start to degrade nearly at 366 C (Figure 3a) and 369 C (Figure 3b), respectively. Some authors [24] have reported the presence of silica particles within the polymer slightly increases its degradation temperature, demonstrating a physical interaction with the polymer chains. Figure 3c shows the epoxy polymer reinforced with cement particles is more stable than the pristine condition and the silica reinforced polymer, starting decomposition nearly at 377 C.

[Figure 3]

In FTIR analysis, many functional groups, such as the C-O bonds, show bands between 1100 and 1230 cm^{-1} [25]. However, wavenumber 1218 cm^{-1} can be attributed to C-C, C-O (stretching) [26] or (C-OH stretching) [27] or (–CH bending) mode (out of plane) [28]. A slight increase in absorption at 1230 cm^{-1} and 1218 cm^{-1} was evidenced when cement particles were incorporated (Figure 4). These results are found in the

reaction of the primary amine with the epoxide to form secondary and tertiary amines that are the main chemical reactions for the epoxy reticulation process [29]. This behaviour can contribute to the increase of crosslink polymeric density which enhances the high mechanical properties of epoxy polymers, such as the compressive strength and stiffness [30].

[Figure 4]

3.3 Experiment II: Hybrid glass fibre reinforced composites (HGFR)

Apparent density (g/cm^3)

The mean apparent density data of the composites varied from 1.644 ± 0.016 to $1.685 \pm 0.011 \text{ g/cm}^3$ (Table 2). Table 3 shows the main factor quartz particle inclusion significantly affected the apparent density of the composites, since a P-value lower than 0.05 was obtained. Figure 5 shows the main effect plot of the particle inclusion on the mean apparent density response. The composites made of cement particle inclusions provided higher apparent density (1.20%) than silica particle inclusions, which can be attributed to the difference in density found for each material. The mean apparent densities for cement and silica particles were measured via gas pycnometer (AccuPyc II 1340 Model) finding 3.12 ± 0.10 and $2.69 \pm 0.02 \text{ g/cm}^3$, respectively.

[Figure 5]

Flexural modulus (GPa)

The mean flexural modulus of the composites varied from 20.39 ± 0.94 to $43.41 \pm 0.66 \text{ GPa}$ (Table 2). The main factors significantly affected the flexural modulus, showing P-values lower than 0.05 (Table 3). Figure 6 presents the main effect plots for the mean flexural modulus. The increasing number of layers provided the increase of composite stiffness, i.e. a change from 7 to 11 layers represented an increase of 56.5% in flexural modulus. The composite thickness is directly related to the area moment of inertia of the beam, consequently, affecting the stiffness of the composites. Silica and cement particle inclusions led to an increasing in flexural modulus of 19.60% and 28.70%, respectively.

[Figure 6]

Flexural strength (MPa)

The mean flexural strength data of the composites varied from 423.12 ± 38.86 to $846.02 \pm 21.78 \text{ MPa}$ (Table 2). Table 3 shows a second order interaction significantly affecting the response. Figure 7 shows the interaction effect plot for the mean flexural

strength response. Higher flexural strengths were achieved when the composites were fabricated with 5wt% of cement particles. The composite strengthening effect by adding particle inclusions is slightly reduced when the number of layers is increased. It is emphasized that 7 layer HGFRC with 5wt% of silica or cement inclusions achieved superior strength compared to 9 layer GFRC. In the same way, 9 layer HGFRC with 5wt% of cement inclusions led to a superior strength compared to 11 layer GFRC. These results reveal that a similar flexural strength can be simultaneously achieved by the reduction of laminate thickness and the incorporation of particles, being able to reduce the final cost of composite structures.

The bending testing combines tensile, compressive and shear loadings. The particles were incorporated only at the upper compressive beam side of the composite. Figure 1 revealed the cement particle inclusions in epoxy polymer were able to increase its compressive modulus by 67%. The flexural strength/stiffness enhancement provided by the particle inclusions can be attributed to (i) the increase in mechanical performance of matrix phase, (ii) the increase in the fracture energy due to the localised plastic shear bands initiated by the stress concentrations around the periphery of the particles, and (iii) the debonding of the microparticles followed by subsequent plastic void growth of the epoxy polymer [11].

[Figure 7]

Impact resistance (J)

HGFRCs fabricated with 11 layers which achieved higher flexural mechanical properties were assessed by impact testing. An Analysis of Variance – One way was considered to evaluate the effect of particle inclusions on the impact resistance. The mean impact energy data for HGFRC varied from 3.33 ± 0.17 to 4.88 ± 0.48 J (Table 2). A P-value of 0.003 revealed the particle inclusions significantly affected this response. $R^2(\text{adj})$ of 97.74% demonstrated the data has good fit to the regression model. Figure 8 shows the main effect plot of particle inclusions for the mean impact resistance. The percent increases of 39.5% and 9.8% in impact resistance was found by adding 5wt% of cement and silica particles, respectively, compared to GFRC. The mean impact resistance of HGFRC with cement particles was 29.7% higher than silica particles.

[Figure 8]

Rahmanian et al. [14] have proposed an energy dissipation mechanism for hybrid particle-fibre composites under impact loading, as follows: (i) strong particles-

fibre and particles-matrix interactions increases fibre-matrix debonding energy, (ii) strong particles-fibre and particles-matrix interactions possess more strength so crack growth requires more energy, and (iii) higher interfacial shear stress transfer between fibre and matrix increases the energy for fibre pull-out. The achievements found in this work implied the physical interactions between cement grains and epoxy polymer were substantially stronger than crystalline quartz particles, leading to a large dissipation of energy, consequently increasing the impact resistance of HGFRCs.

Microstructural analysis

Figure 9 shows the backscattering electron images of fracture surfaces after flexural testing. The composites consisted of cement particles provided less damage on the compressive side (Figure 9a) and greater damage on the tensile side of the beam (Figure 9b) compared to those composites reinforced with silica particles, see Figure 7c (compressive side) and Figure 9d (tensile side). This behaviour can be attributed to the higher compressive stiffness achieved by cement particle inclusions at the upper side of the beam. The crack configuration found in the compressive side of cement reinforced composites (Figure 9a) looks more brittle than that shown by silica reinforced composites (Figure 9b), which reveals a wider crack. Figure 4 indicated the flexural modulus of HGFRC made with 5wt% of cement particles was 9.1% higher than those made of 5wt% of silica particles, revealing a significant difference in stiffness.

[Figure 9]

4. Conclusions

In general, the compressive modulus of epoxy resin increased by adding silica or cement particles. A major percent increase of 67% was achieved when 5wt% of cement particles were incorporated. This behaviour was attributed to the cross-linked effect within the epoxy polymer, as revealed by TGA and FTIR analyses. The thermal decomposition temperatures were increased by adding ceramic particles into the epoxy polymer, mainly when cement particles were incorporated. The apparent density of HGFRCs increased by 0.62% and 1.82% when silica and cement particles were added at the upper beam side, respectively. The increasing number of layers, i.e. from 7 to 11 layers, provided a percent increase of 56.5% in composite stiffness. Silica and cement particle inclusions, at the upper beam side, led to an increasing in flexural modulus of 19.60% and 28.70%, respectively. The highest flexural strength was achieved when the HGFRCs were fabricated with 5wt% of cement particles. Similar flexural strength can

be simultaneously achieved by the reduction of laminate thickness and the incorporation of particles, being able to reduce the final cost of composite structures. The percent increases of 39.5% and 9.8% in impact resistance was found by adding 5wt% of cement and silica particles, respectively. The mean impact resistance of HGFRCs with cement particles was 29.7% higher than silica particles. HGFRCs made with cement inclusions revealed a trend of brittle fracture mode compared to those made with silica particles. Hybrid “cross-ply” glass fibre composite will be the scope of future investigations specially to verify if the interlocking effect, due to the presence of particles at the interlaminar region, is enhanced by the 90° fibre orientation.

Acknowledgments

The authors would like to thank the Brazilian Research Agencies, CNPq and FAPEMIG for the financial support provided.

References

- [1] B. Wetzel, F. Hauptert and M.Q. Zhang. *Compos. Sci. Technol.*, **63**, 14 (2003).
- [2] H. Ghasemnejad, A. S. M. Furquan and Mason, P. J. *Materials & Design*, **31**, 8 (2010).
- [3] C. M. Manjunatha, A. C. Taylor, A. J. Kinloch and S. Sprenger. *Composites Science and Technology*, **70**, 1 (2010).
- [4] F.A. López, M.I. Martín, F.J. Alguacil, J. Ma. Rincón, T.A. Centeno, M. Romero. *Journal of Analytical and Applied Pyrolysis*, **93** (2012).
- [5] Y. Cao and J. Cameron. *Journal of Reinforced Plastics and Composites*, **25**, 7 (2006).
- [6] S. Markkula, H. C. Malecki and M. Zupan. *Composite Structures*, **95** (2013).
- [7] J. L. Abot, Y. Song, M. J. Schulz and V. N. Shanov. *Composites Science and Technology*, **68**, 13 (2008).
- [8] M. Rajanish, N.V. Nanjundaradhya and R. S. Sharma. *Procedia Materials Science*, **10** (2015).

- [9] J. C. Santos, L. M. G. Vieira, T. H. Panzera, M. A. Schiavon, A. L. Christoforo and F. Scarpa. *Materials & Design*, **65** (2015).
- [10] T.H. Hsieh, A.J. Kinloch, K. Masania, A.C. Taylor and S. Sprenger. *Polymer*, **51**, 26 (2010).
- [11] Y. Zheng, R. Ning and Y. Zheng. *Journal of Reinforced Plastics and Composites*, **24**, 3 (2005).
- [12] J. Tsai and Y. Cheng. *Journal of Composites Materials*, **43** (2009).
- [13] L. M. G. Vieira, J. C. Santos, T. H. Panzera, A. L. Christoforo, V. Mano, J. C. C. Rubio and F. Scarpa. *Polymer Composites*, (2016).
- [14] S. Rahmanian, K. S. Thean, A. R. Suraya, M. A. Shazed, M. A. Mohd Salleh and H. M. Yusoff. *Materials & Design*, **43** (2013).
- [15] A. C. Detomi, R. M. Santos, S. M.R. Filho, C. C. Martuscelli, T. H. Panzera and F. Scarpa. *Materials & Design*, **55** (2014).
- [16] T. H. Panzera, A. L. R. Sabariz, K. Strecker, P. H. R. Borges, D. C. L. Vasconcelos and W. L. Wasconcelos. *Cerâmica*, **56** (2010).
- [17] ASTM Standard D695. “Standard Test Method for Compressive Properties of Rigid Plastics”, ASTM International, West Conshohocken, PA (2010). doi:10.1520/D0695-10.2.
- [18] BS 8110-1. Structural use of concrete Part 1: Code of practice for design and construction (1997).
- [19] C. F. Jeff Wu and Michael S. Hamada, M. *Experiments: Planning, Analysis, and Parameter Optimization*, John Wiley & Sons, New York (2000).
- [20] ASTM Standard D790-15e2 “Standard Test Methods for Flexural Properties of Unreinforced and Reinforced Plastics and Electrical Insulating Materials,” ASTM International, West Conshohocken, PA (2010), DOI: 10.1520/D0790-15E02.
- [21] ASTM Standard D6110 – 10 “Standard b Test Method for Determining the Charpy Impact Resistance of Notched Specimens of Plastics”. ASTM International, West Conshohocken, PA (2010), DOI: 10.1520/ D6110-10

- [22] ASTM Standard D792. “Standard Test Methods for Density and Specific Gravity (Relative Density) of Plastics”, ASTM International, West Conshohocken, PA (2008). doi:10.1520/D0792-08.2
- [23] J. Chen, C. K. Ober, M. D. Poliks, Y. Zhang, U. Wiesner and C. Cohen. *Polymer* **45** (2004).
- [24] Y. Liu, J. Chen, G. Li, X. Liu, X. Liao, Q.i. *J. Appl. Polym. Sci.* **131**, 20 (2014).
- [25] B. C. Smith. *Infrared Spectral Interpretation: A Systematic Approach*. CRC Press, p.93 (1998)
- [26] J. C. del Rio, A. Gutiérrez, I. M. Rodríguez, D. Ibarra and Á. T. Martínez. *J. Anal. Appl. Pyrolysis*, **79** (2007).
- [27] W. J. Basirun, M. Sookhakian, S. Baradaran, M. R Mahmoudian and M. Ebadi. *Nanoscale Research Letters*, **8**, 397 (2013).
- [28] S.M. Asharaf, S. Ahmad and U. Riaz. *A Laboratory Manual of Polymers*. I. K. International Pvt Ltd, p.34 (2008).
- [29] G. Nikolic, S. Zlatkovic, Mc Cakic, S. Cakic, C. Lacnjevac and Z. Rajic. *Sensors*, **10** (2010).
- [30] R. Shih, S. Kuo and F. *Polymer*, **52**, 3 (2011).

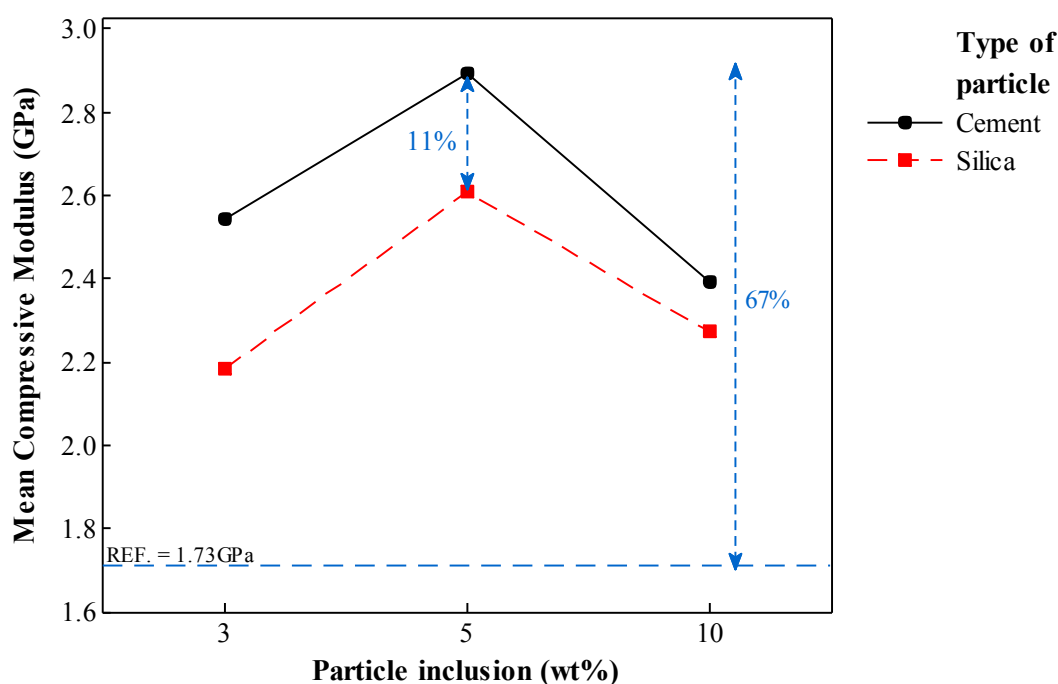


Figure 1. Interaction effect plot for compressive modulus

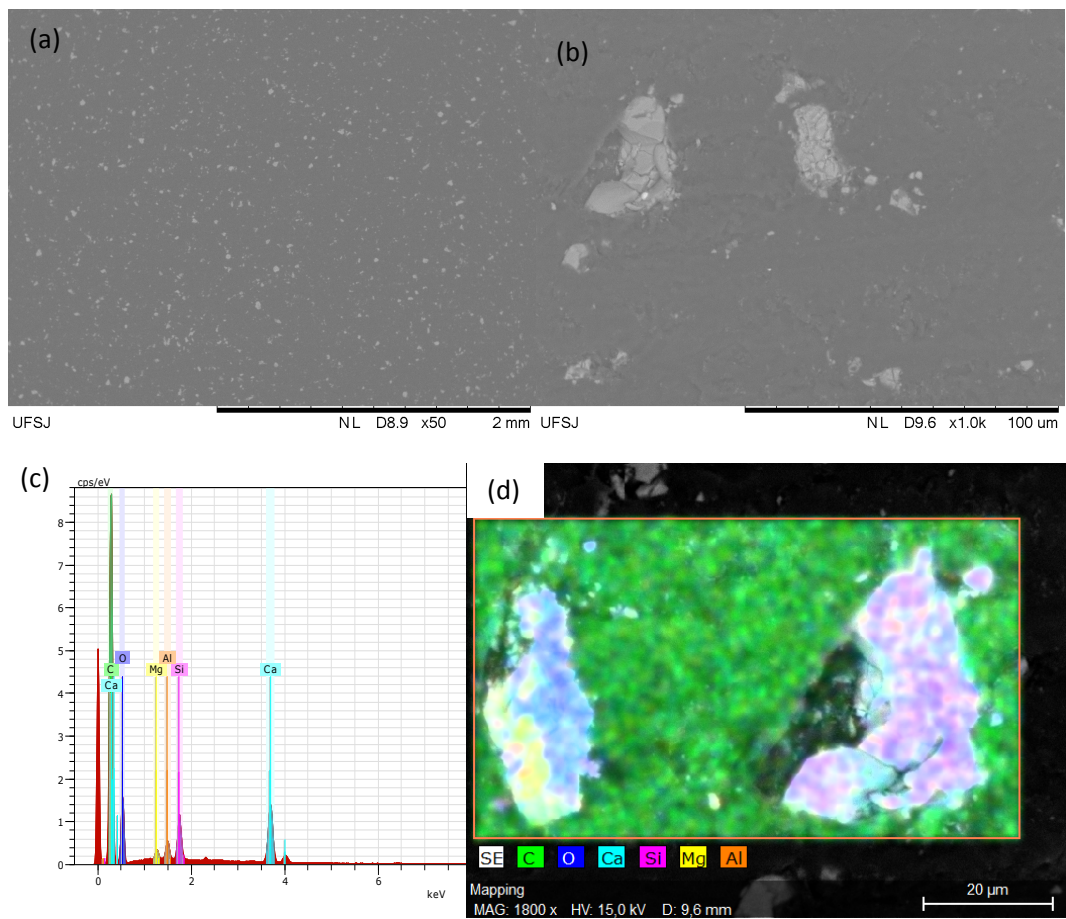
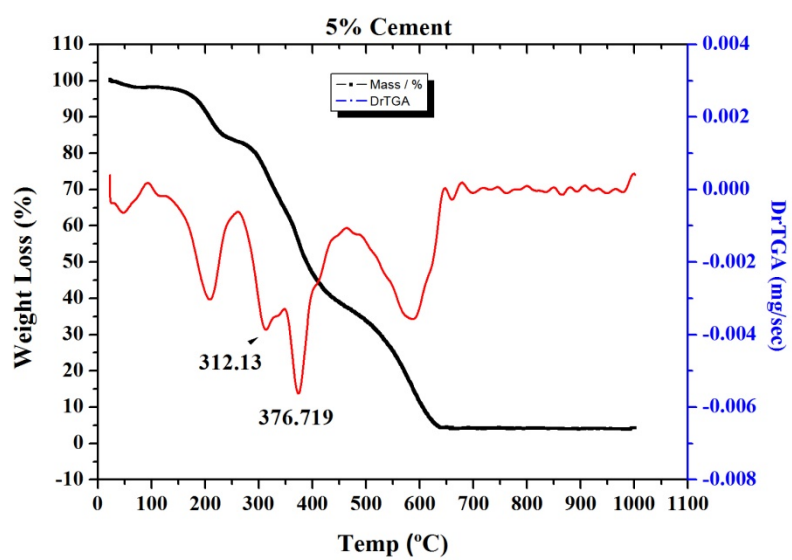
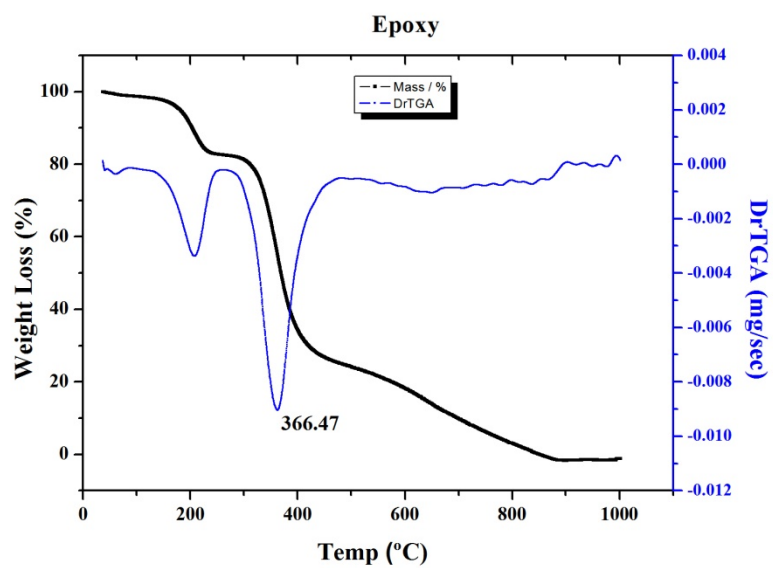


Figure 2. Scanning electron microscopy images (a, b) with X-ray microanalysis (c, d).



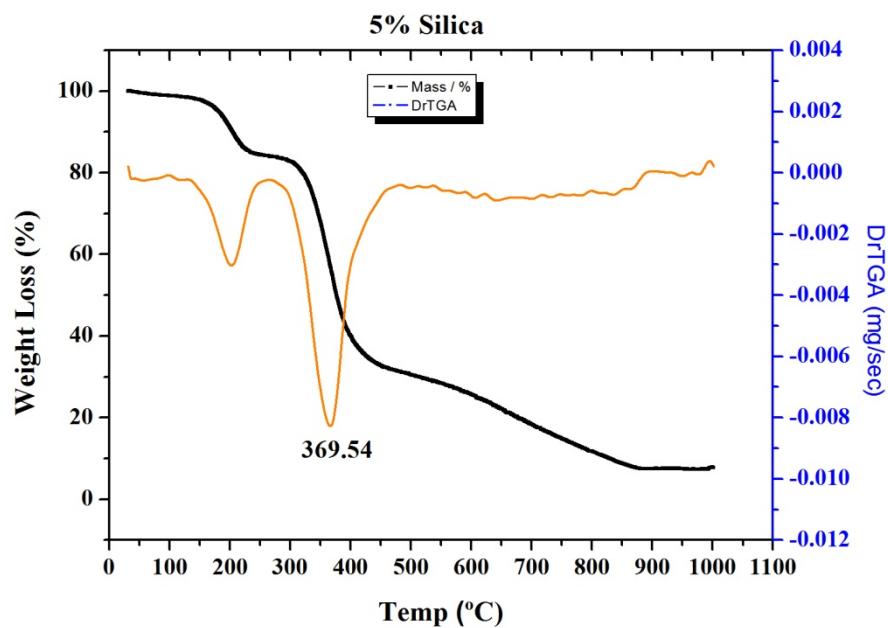


Figure 3. TGA curves for the pristine epoxy (a) with 5% of silica (b) and 5% of cement (c).

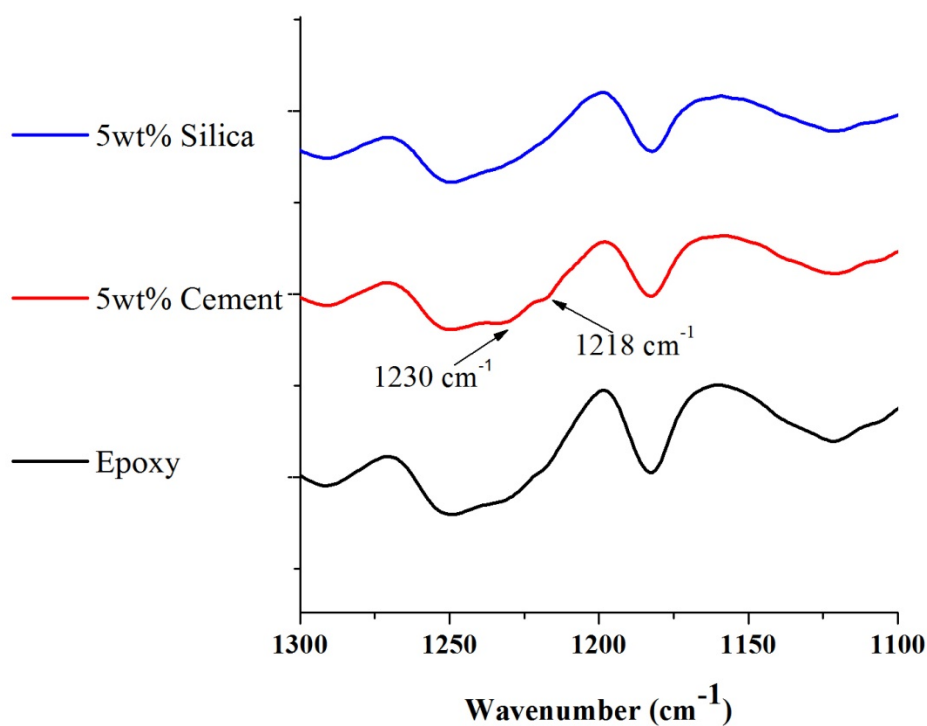


Figure 4. Fourier transform infrared spectroscopy (FTIR) analyses.

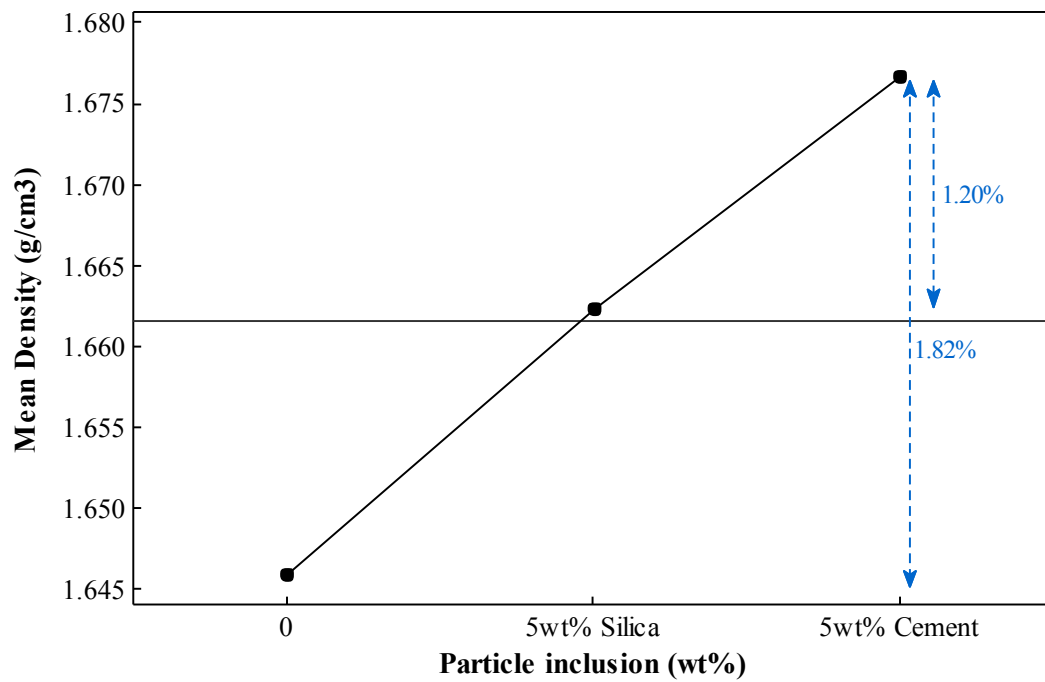


Figure 5. Main effect plot of the particle inclusion on the mean apparent density response.

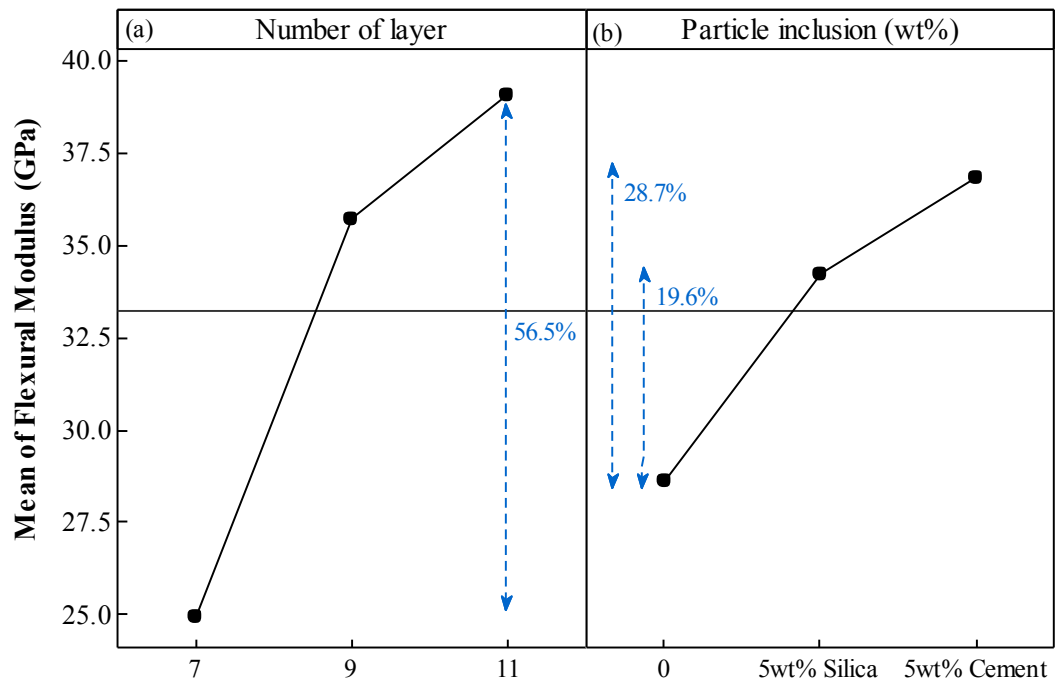


Figure 6. Main effect plots for the mean flexural modulus response.

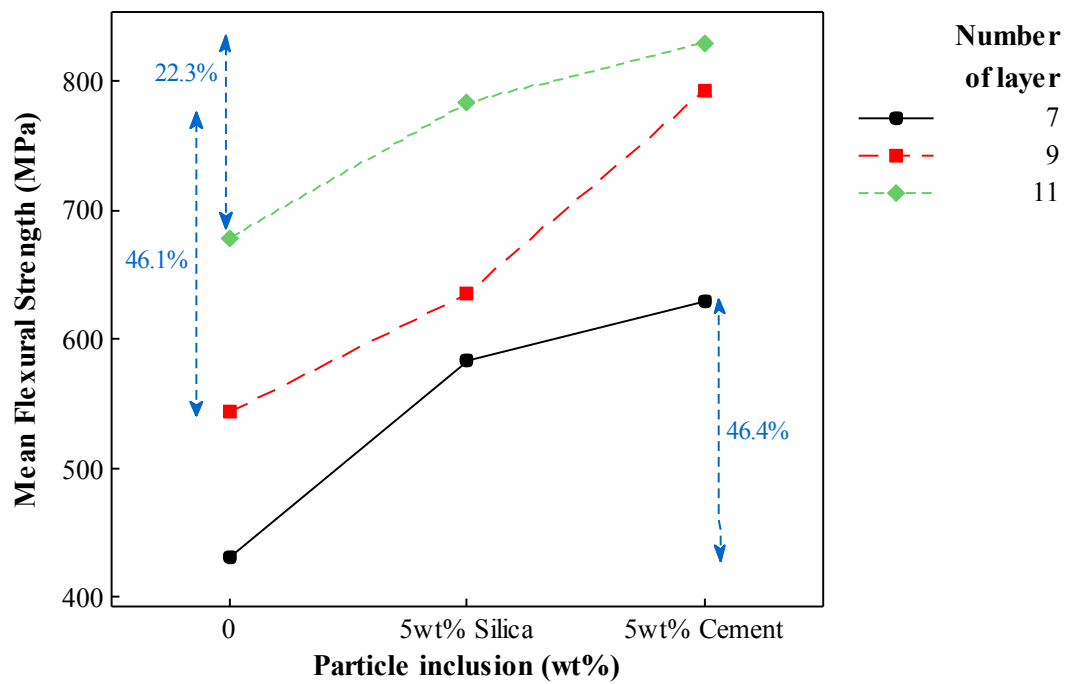


Figure 7. Interaction effect plots for the mean flexural strength response.

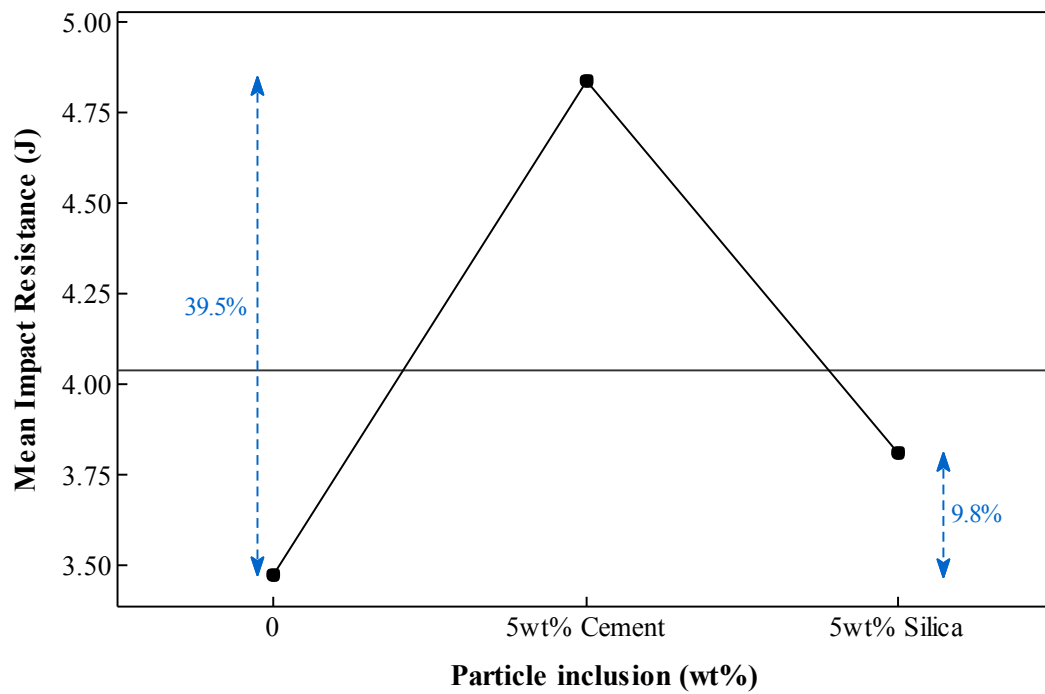


Figure 8. Main effect plot for the mean impact resistance.

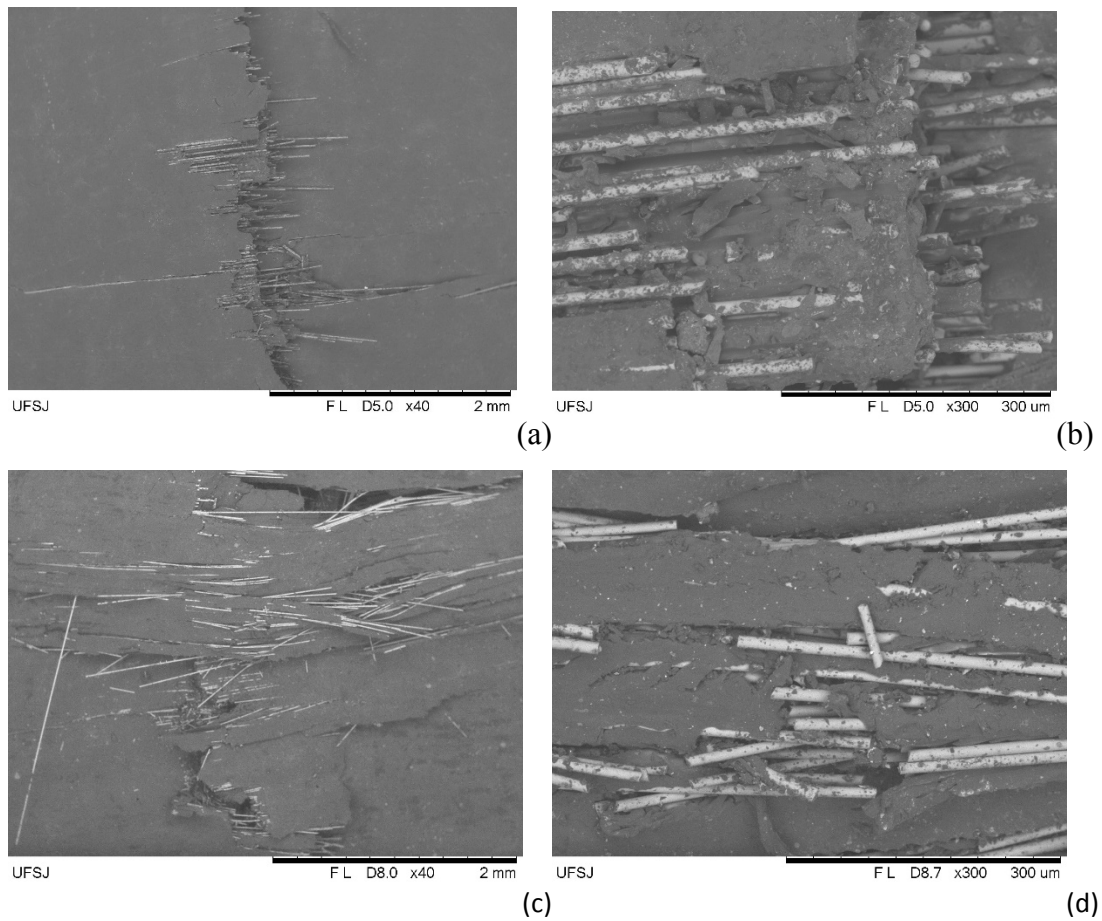


Figure 9. SEM images, fracture mode of HGFRc: with cement inclusions at (a) compressive side - 40 \times and (b) at tensile side - 300 \times , and with silica inclusions at (c) compressive side - 40 \times and (d) tensile side - 300 \times .